(2)

WL-TR-91-2047

HIGH EFFICIENCY GaAs/Ge MONOLITHIC TANDEM CELLS FOR SPACE CONCENTRATOR ARRAYS

Steven J. Wojtczuk

Spire Corporation
Patriots Park
Bedford MA 01730

May 1991

Interim Report for Period August 1988 - August 1989

AERO PROPULSION & POWER DIRECTORATE
WRIGHT LABORATORY
AIR FORCE SYSTEMS COMMAND
WRIGHT-PATTERSON AIR FORCE BASE, OHIO 45433-6563

NOTICE

When Government drawings, specifications, or other data are used for any purpose other than in connection with a definitely Government-related procurement, the United States Government incurs no responsibility or any obligation whatsoever. The fact that the government may have formulated or in any way supplied the said drawings, specifications, or other data, is not to be regarded by implication, or otherwise in any manner construed, as licensing the holder, or any other person or corporation; or as conveying any rights or permission to manufacture, use, or sell any patented invention that may in any way be related thereto.

This report is releasable to the National Technical Information Service (NTIS). At NTIS, it will be available to the general public, including foreign nations.

This technical report has been reviewed and is approved for publication.

JAMES D. SCOFIELD, Project Engineer

LOWELL D. MASSIE, Chief
Power Components Branch
WL/POOC

FOR THE COMMANDER

MICHAEL D. BRAYDICH, Lt Col, USAF
Chief, Director
Aerospace Power Division
Aero Propulsion & Power Directorate

If your address has changed, if you wish to be removed from our mailing list, or if the addressee is no longer employed by your organization please notify WL/POOC, WPAFB, OH 45433-6563 to help us maintain a current mailing list.

Copies of this report should not be returned unless return is required by security considerations, contractual obligations, or notice on a specific document.

UNCLASSIFIED
SECURITY CLASSIFICATION OF THIS PAGE

REPORT DOCUMENTATION PAGE

Form Approved OMB No. 0704-0188

1a. REPORT SECURITY CLASSIFICATION UNCLASSIFIED	1b. RESTRICTIVE MARKINGS
2a. SECURITY CLASSIFICATION AUTHORITY	3. DISTRIBUTION/AVAILABILITY OF REPORT Approved for public release; distribution is unlimited.
2b. DECLASSIFICATION/DOWNGRADING SCHEDULE	
4. PERFORMING ORGANIZATION REPORT NUMBER(S)	5. MONITORING ORGANIZATION REPORT NUMBER(S) WL-TR-91-2047
6a. NAME OF PERFORMING ORGANIZATION Spire Corp. — 6b. OFFICE SYMBOL (*If applicable*)	7a. NAME OF MONITORING ORGANIZATION Aero Propulsion and Power Dir. (WL/POOC) Wright Laboratory
6c. ADDRESS (*City, State, and ZIP Code*) Patriots Park Bedford MA 01730	7b. ADDRESS (*City, State, and ZIP Code*) Wright-Patterson AFB OH 45433-6563
8a. NAME OF FUNDING/SPONSORING ORGANIZATION WL/POOC — 8b. OFFICE SYMBOL (*If applicable*)	9. PROCUREMENT INSTRUMENT IDENTIFICATION NUMBER F33615-88-C-2844
8c. ADDRESS (*City, State, and ZIP Code*) WPAFB OH 45433-6563	10. SOURCE OF FUNDING NUMBERS

PROGRAM ELEMENT NO.	PROJECT NO.	TASK NO.	WORK UNIT ACCESSION NO.
63224F	L210	00	04

11. TITLE (*Include Security Classification*)

High Efficiency GaAs/Ge Monolithic Tandem Cells for Space Concentrator Arrays

12. PERSONAL AUTHOR(S)
Steven J. Wojtczuk

13a. TYPE OF REPORT	13b. TIME COVERED	14. DATE OF REPORT (*Year, Month, Day*)	15. PAGE COUNT
Interim	FROM Aug 88 TO Aug 89	May 1991	21

16. SUPPLEMENTARY NOTATION
This effort was accomplished under PRDA 88-01 Competitive Selection Award

17. COSATI CODES			18. SUBJECT TERMS (*Continue on reverse if necessary and identify by block number*)
FIELD	GROUP	SUB-GROUP	Multi-junction, concentrator, high temp, monolithic, tandem
1001	2202	2012	

19. ABSTRACT (*Continue on reverse if necessary and identify by block number*)

The goal of this program is to develop a 30 percent efficient 2-junction solar cell that is monolithic, two terminal, and that will operate in 25-100x solar concentrator elements with operating temperatures of 75-100°C. The cell design is a GaAs/Ge compound configuration with the Ge bottom cell utilizing the .9-1.8 micron portion of the AMØ solar spectrum and contributing 7 percent to the total stack efficiency.

During the first Phase of this effort individual component cells were developed that had efficiencies of 22% for GaAs and 6% for Ge. Monolithically grown 2-junction devices were also fabricated with efficiencies exceeding 20% when characterized at the defined operating temperatures and solar concentration.

20. DISTRIBUTION/AVAILABILITY OF ABSTRACT	21. ABSTRACT SECURITY CLASSIFICATION
☐ UNCLASSIFIED/UNLIMITED ☐ SAME AS RPT ☒ DTIC USERS	UNCLASSIFIED

22a. NAME OF RESPONSIBLE INDIVIDUAL	22b. TELEPHONE (*Include Area Code*)	22c. OFFICE SYMBOL
JAMES D. SCOFIELD	513-255-5925	WL/POOC

DD Form 1473, JUN 86 *Previous editions are obsolete*

4 April 1990
Phase 1 Interim Report - 10115
Report Period: August 1988
September 1989

CONTRACT TITLE AND NUMBER:

HIGH EFFICIENCY GaAs/Ge MONOLITHIC TANDEM CELLS FOR SPACE CONCENTRATOR ARRAYS; F33615-88-C-2844

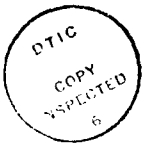

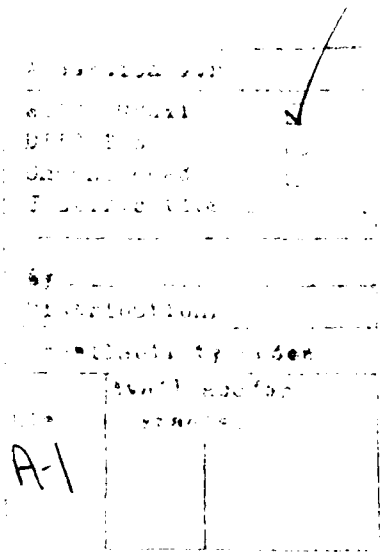

CONTRACTING AGENCY:

WRDC/POOC-2
Wright-Patterson Air Force Base
Ohio 45433-6563

CONTRACTOR'S NAME AND ADDRESS:

Spire Corporation
Patriots Park
Bedford, MA 01730

CONTRACT PERIOD: 10 August 1988 to 9 December 1991

SUMMARY:

GaAs/Ge monolithic tandem two-junction concentrators are being developed by optimizing separate one-junction GaAs and Ge cells which simulate the GaAs top cell and Ge bottom cell of the tandem. Separation allows easier analysis of the tandem's top and bottom cells than if these two junctions were in series.

GaAs top cells fabricated in Phase 1 had a (wafer average) 100X AM0 efficiency of 22.1% at 80°C, exceeding the Phase 1 goal of 22%.

Ge bottom cells studied have a GaAs optical filter (but no GaAs junction) to replicate the spectrum the Ge cell sees when incorporated into a tandem. Wafer average Ge-under-GaAs bottom cell efficiency is 3.8% at 80°C 100X AM0, again exceeding the Phase 1 goal of 3%. We found further evidence that the 900-1800 nm response seen from the Ge bottom cell is due to a p-n junction in the Ge, and not a GaAs/Ge heterojunction.

Tandem cells at 30X AM0 and 80°C had efficiencies of about 20.2%, versus the Phase 1 goal of 24% at 100X AM0. We could not achieve the required concentration of 100X, where the efficiency may have been better, because our plastic concentrating optics absorbed the IR light. Small off-axis parabolic mirrors were used to uniformly concentrate the light spectrum. Although the Ge bottom cell exceeded the Phase 1 goal of 3%, it is limiting the tandem cell efficiency and degrading the fill factor by limiting the tandem cell current. Higher Ge bottom cell efficiencies (about the 7% called for at the end of Phase 2) are needed.

1.0 INTRODUCTION

GaAs/Ge monolithic tandem cells present a unique blend of characteristics desirable for high efficiency space cells. First, the bandgaps of GaAs and Ge (1.42 and 0.67 eV) are such that a large amount (theoretically 36%) of the power in the solar spectrum can be utilized by the tandem.[1] Secondly, the theoretical photocurrents generated by a GaAs cell and a Ge-under-GaAs cell under AM0 are almost matched, allowing efficient use of simpler two-terminal tandems. Thirdly, GaAs and Ge technology are relatively well developed. GaAs technology is widely used in space applications because of its radiation-hardness compared to silicon, while Ge technology was developed during the infancy of semiconductors. Finally, Ge substrates have many desirable properties for tandem cell space applications.[2] Lattice constants and thermal expansion coefficients of Ge and GaAs are closely matched, allowing problem-free growth of monolithic tandems. Ge substrates are less expensive, better thermal conductors, and stronger mechanically than GaAs substrates. This allows the use of thinner and lighter wafers, a critical factor in one-sun space applications.

These desirable properties spurred recent efforts to develop GaAs/Ge tandems.[1-5] However, development is hampered by difficulties in measuring tandem efficiency accurately.[6,7] Tandems require a more accurate solar simulator spectrum than one-junction cells need, since the source spectrum determines which of the two junctions limits cell efficiency. Most reliable AM0 results are currently from aircraft-flown GaAs/Ge cells.[8] Part of our motivation for the separation of the monolithic two-junction tandem into single-junction GaAs top cells and single-junction Ge bottom cells is to perform accurate measurements with current test equipment, until our tandem cell test equipment is developed. Difficulties in extracting top and bottom cell

parameters from tandem data provide the remaining motivation. Analyzing and optimizing single-junction top and bottom cells is a more tractable problem than analyzing a tandem, where the number of unknown parameters is about doubled In this program we are utilizing a design approach illustrated in Figure 1.

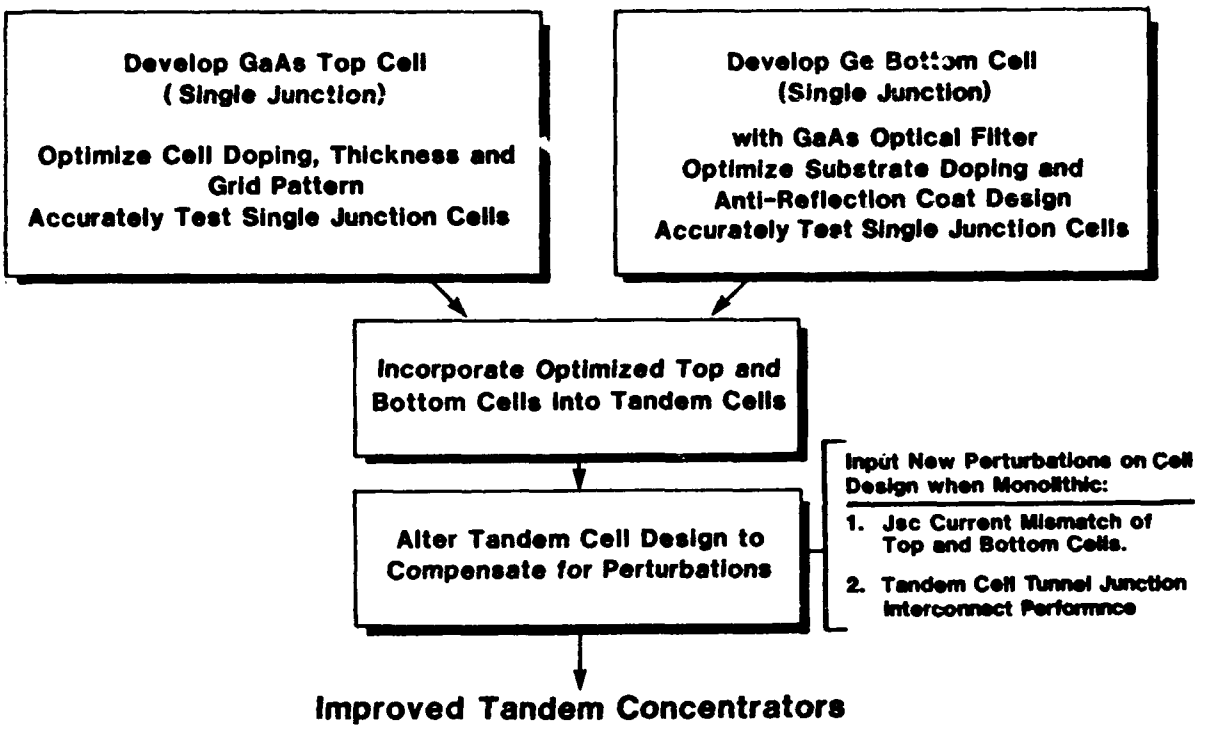

FIGURE 1. TANDEM CELL DEVELOPMENT FLOW DIAGRAM.

2.0 DEVICE STRUCTURES AND FABRICATION

All of the cell structures were grown by metalorganic chemical vapor deposition (MOCVD) using a commercial Spire SPI-MO CVD^{TM} 450 atmospheric pressure epitaxial reactor. Reactants were TMGa, TMAl, and AsH_3. Dopants were SiH_4 (N) and DMZn (P). Growth temperature for all layers was 740°C except for the GaAs cap (700°C). The V/III ratio was 15:1. Growth rates were about 4 microns/hour.

Two-inch Sb-doped n-type Ge substrates from Eagle-Picher, Hobokenand Cominco were used, with resistivities from 18 to 50 milliohm-cm. All Ge wafers were about 450 microns thick. Both the Hitachi GaAs and the Ge wafers used were oriented 2° off (100) to aid in better crystal growth. The back sides of the Ge substrates were coated with GaAs prior to growth of the cells in Figure 2 to prevent any possible autodoping effects. GaAs caps on the Ge wafer backsides were removed after growths.

Figure 2a illustrates a typical Spire tandem cell, while Figures 2b and 2c show the GaAs top cell and Ge bottom cells used in the optimization and development. Two different structures were used in experiments to discern whether the photoresponse from the bottom cell is due to a p-n Ge junction or a GaAs/Ge heterojunction, which is a subject of current research debate. This experiment is discussed in Section 4, but the important result was evidence indicating the 900-1800 nm response of our GaAs/Ge tandems is due to a Ge p-n junction and not a heterojunction.

This p-n junction in the Ge is created by diffusion of Ga and As into the Ge during the GaAs cell growth. At the growth temperature, Ga has a higher solid solubility limit ($5 \times 10^{20}/cm^3$) than As ($2 \times 10^{20}/cm^3$).[9] Also, Ga has a much lower diffusion coefficient at 740°C (about 10^{-14} cm^2/s) than As (about 5×10^{-12} cm^2/s).[10] Therefore, the p-type dopant Ga diffuses into the Ge a shorter distance during the 90 minute growth, compensating the diffusing As from the GaAs and already present Sb in the Ge wafer, both n-type dopants. The result is a shallow p-n Ge junction just below the GaAs epilayer.

The theoretical diffusion length for the Ga in Ge using the above numbers is $(Dt)^{1/2}$ or 0.073 microns. The As diffusion length is 1.6 microns and the As background is much greater than the Sb dopant in the Ge for several microns. Assuming a constant surface concentration of Ga from the GaAs at the GaAs/Ge interface, and that the Ge doping is due to As at the solid solubility limit, the junction depth calculated from a complementary error function curve is 0.1 micron. Actual junctions depths have been measured for 700°C growths by spreading resistance measurements (0.1 micron) [1] and for 740°C growths by electron beam induced current (EBIC) (0.4 microns).[11] This rough agreement is all we believe can be expected since the diffusion constants at the Ge/GaAs interface are probably somewhat different than the published values. Another indication of the Ge junction is the higher Voc of our GaAs/Ge cells, typically 1.2 volts,[1,5] compared to about 1 volt for typical GaAs cells.

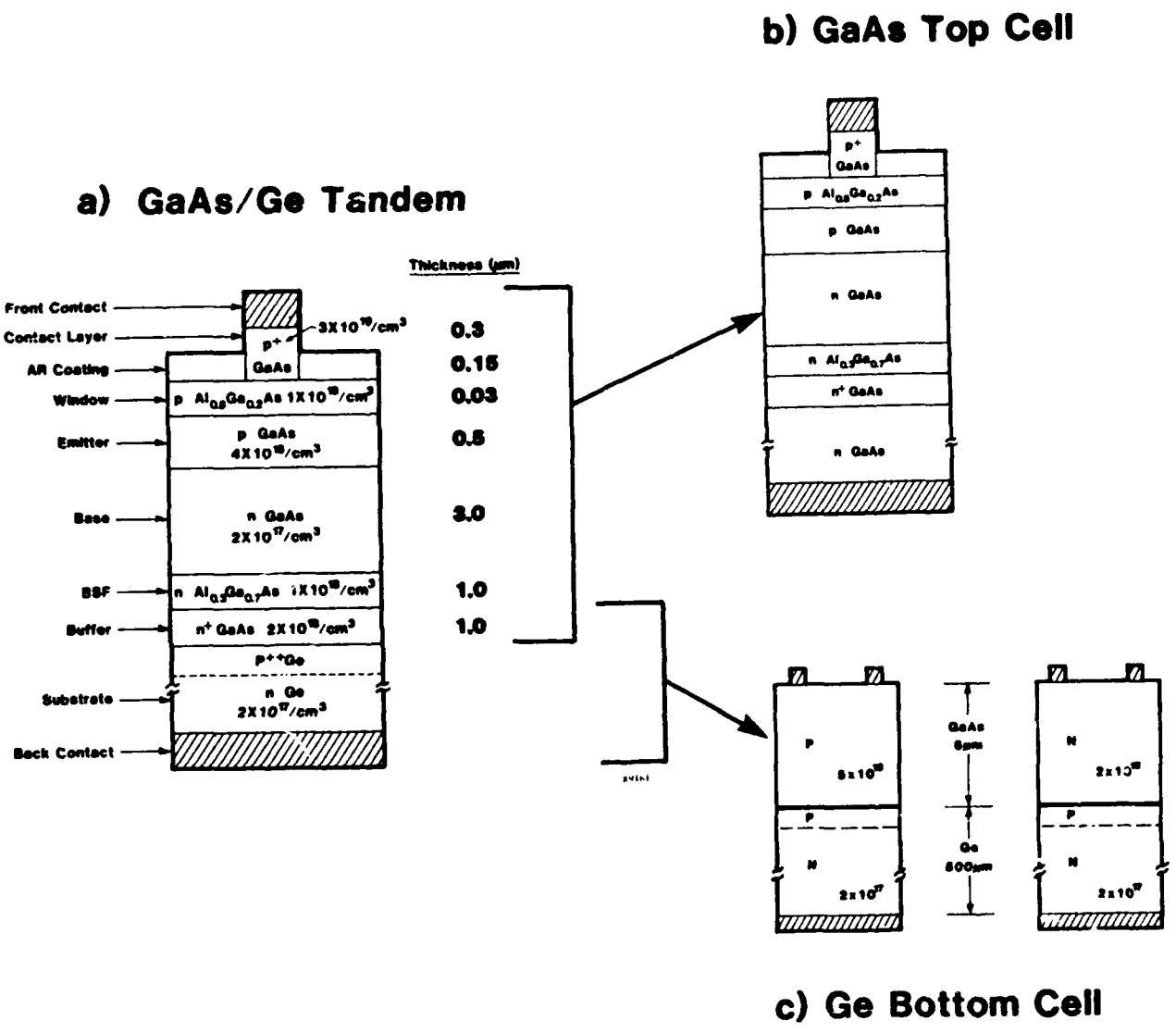

FIGURE 2. EVOLUTION OF GaAs TOP CELL (b) AND Ge-UNDER-GaAs BOTTOM CELL (c) FROM A MONOLITHIC TANDEM CELL (a).

Solar cells were fabricated as follows. First, wafer fronts were protected with a SiO_2 coat. Wafer backs were etched for several microns and then either 2500 angstroms AuGe/2500 angstroms Au (GaAs top cell wafer) or 1000 angstroms Au/5000A Ag (Ge bottom cell wafers) was thermally evaporated on the backs. Wafers were then sintered at 450°C for 5 min (GaAs) or 375°C for 5 min (Ge). Next, the grid pattern was photolithographically defined on the fronts using an image reversal process to obtain a resist profile suitable for liftoff, and the oxide was etched in the grid. Then either 400 angstroms Cr/3 microns Au (GaAs top cell) or 1000 angstroms AuGe/3 microns Ag (N GaAs on Ge bottom cell, Figure 2c) or 500 angstroms Cr/500 angstroms Au/3 microns Ag (P GaAs on Ge bottom cell, Figure 2c) was e-beam evaporated onto the fronts. Excess metal was lifted off in acetone, and then the contacts were sintered. Next, mesas were defined photolithographically around the cell, developed, and etched. The oxide and the GaAs cap layer between the front grid fingers was then etched away. Finally, an AR coating of 500 angstroms ZnS/1000 angstroms MgF_2 (GaAs top cells) or 900 angstroms ZnS/1500 angstroms MgF_2 (Ge bottom cells) was thermally evaporated. One of the Ge bottom cell runs (#5209) discussed in Section 4 received the wrong AR coating and so has somewhat lower J_{SC}'s and efficiencies than the other bottom cells.

3.0 GaAs TOP CELL

GaAs concentrator cells were fabricated which are the most efficient reported to date at AM1.5D without prismatic covers (28.7% AM1.5D) and exceeding the Phase 1 goal at 22.1% 100X AM0 average at 80C (24.5% AM0 at 25C). Figure 3 depicts the GaAs top cell, whose cross-section is shown in Figure 2. The busbar and cell junction area are coincident squares with 5 mm sides. The cell diameter is set by the space system considerations to 4 mm (photoactive area 0.126 cm^2). Dopings and thicknesses in Figure 2 are similar to Spire's standard GaAs high efficiency one-sun cells.[1,5,12] Two rectangular patterns in the upper left corner by each cell in Figure 3 are contact transmission line test patterns. Monitoring these structures at selected steps during cell processing allows measurement of GaAs cap sheet resistance, contact resistivity and GaAs emitter sheet resistance across the wafer. Each cell also has a small diode visible at its upper right in Figure 3 for CV measurement of the GaAs base doping.

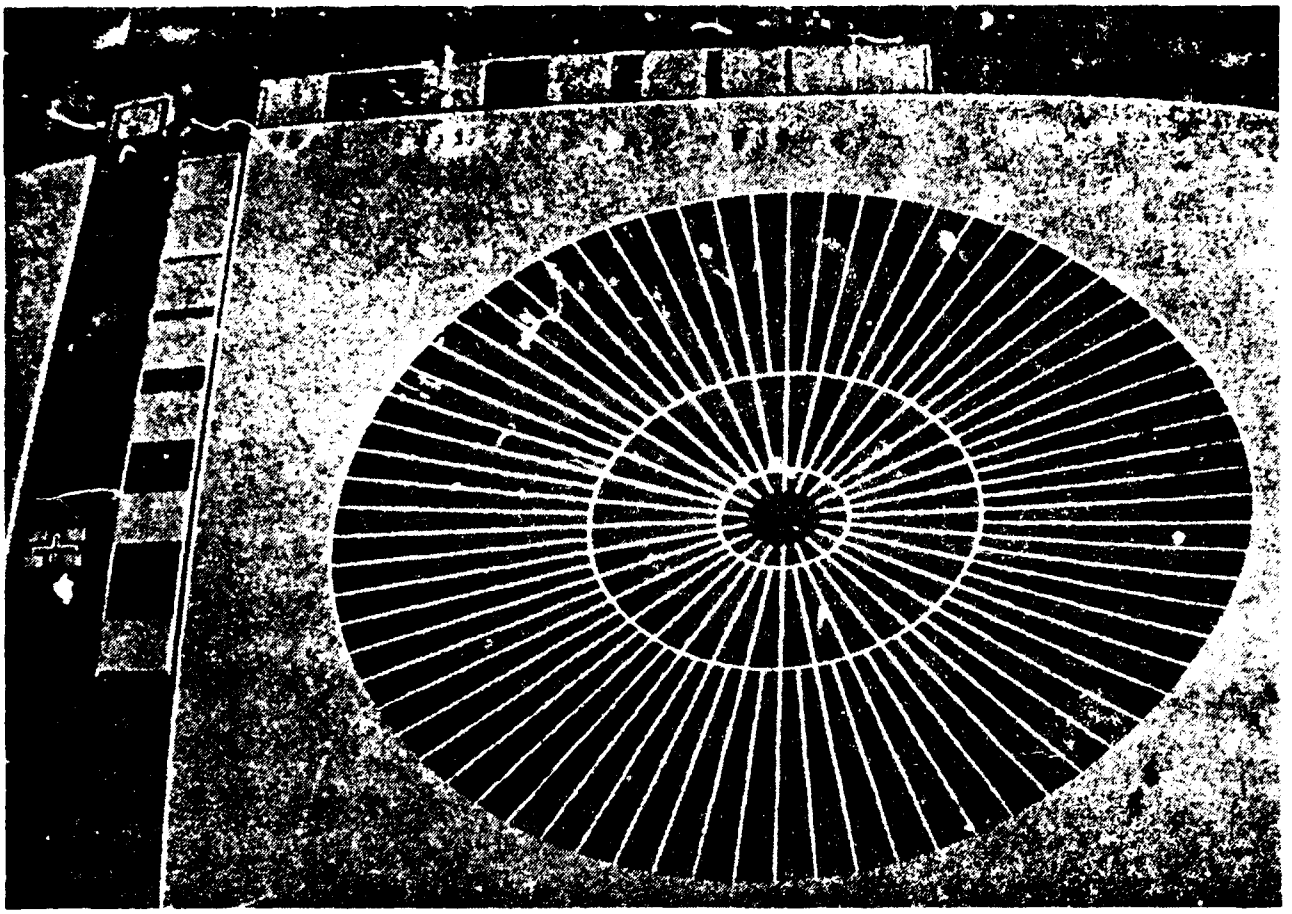

FIGURE 3. GaAs TOP CELL CONCENTRATOR. Busbar and junction are coincident squares 5 mm on a side. Photoactive area is 0.126 cm^2 (4 mm diameter). Shadow is 4.6%.

Best cell efficiencies measured by Sandia National Laboratories are show in Figure 4. It was assumed in setting the concentration ratio that the short-circuit current density (J_{sc}) was linear with intensity, which is valid for most high-efficiency GaAs cells. The one-sun AM1.5D J_{sc}'s were measured with a Si reference cell using a spectral mismatch correction. The AM0 25°C J_{sc} was measured with a GaAs reference cell. The AM0 80C J_{sc} was calculated using temperature coefficients measured by the Solar Energy Research Institute on similar cells. Sandia measured a higher one-sun AM1.5D J_{sc} than Spire (see Table 1), and therefore a higher efficiency at AM1.5D. However, AM0 measurements are in good agreement. Since Sandia serves as the U.S. national standards lab for concentrator measurements, we are emphasizing their measurements. However, we will discuss the discrepancy.

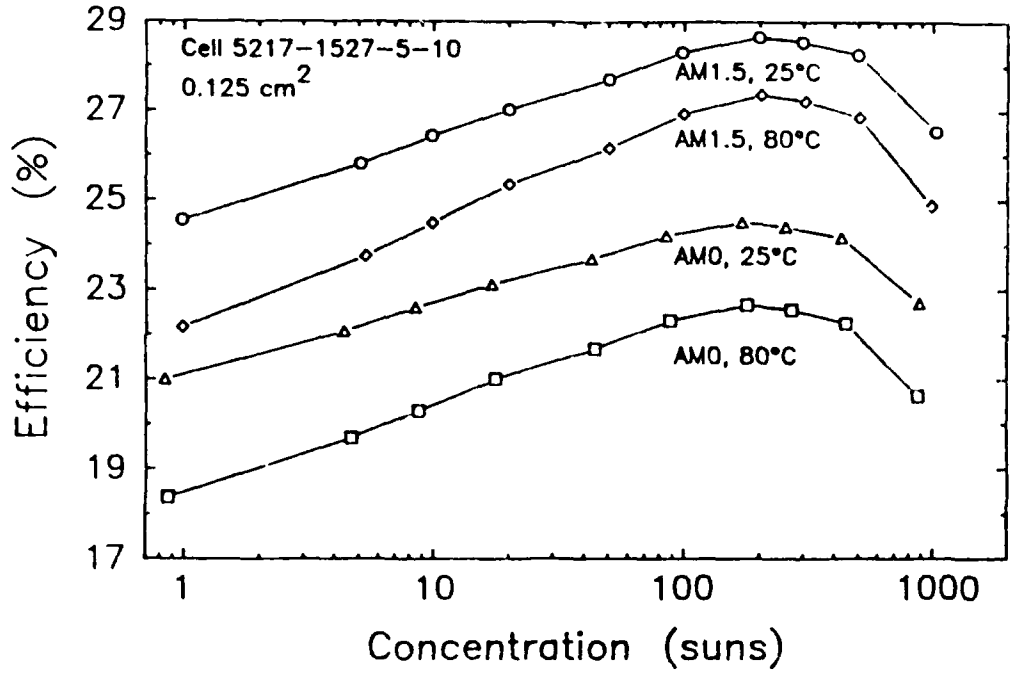

FIGURE 4. SOLAR EFFICIENCY OF BEST SPIRE GaAs CELL AS MEASURED BY SANDIA.

TABLE 1. COMPARISON OF MEASURED GaAs TOP CELL ONE-SUN J_{sc} (mA/cm^2).

Spectrum	Cell #	Spire Simulator	Spectral Response	Sandia Simulator	Spectral Response
AMO	10	32.92	33.22	33.61	33.42
AM1.5D	10	25.72	26.79	28.75	26.16

Sandia used a NASA-calibrated Si reference cell to set the intensity of a Spectrolab XT-10 simulator. A spectral mismatch correction of 0.977 gives a one-sun J_{sc} of 28.75 mA/cm^2. Spire used a JPL-calibrated Si reference and a Spectrolab X-25 simulator with a spectral mismatch of 1.035, giving a one-sun J_{sc} of 25.72 mA/cm^2. The 12% difference is much larger than expected from reference cell calibration errors. Convolving the absolute spectral response curves measured by Sandia and Spire with the reference AM1.5 direct spectrum[13] gave J_{sc}'s of 26.16 and 26.79 mA/cm^2, respectively, intermediate between the simulator values. It is therefore not clear which is the true efficiency under AM1.5 conditions. However, Sandia's reference cell has been used to measure other high-efficiency concentrator cells,[14,15] and so should give a good relative comparison to those results. Sandia also finds that its calibration agrees with outdoor efficiency measurements in Albuquerque, NM.

Since the cells had such high efficiencies, we will discuss the grid design briefly. Grid finger width, number of current-sharing rings, and the finger reduction factor between zones are set to convenient near-optimum values. All grid lines are 3 microns wide, our current photolithographic limit. The number of current-sharing rings is set to three.[16] The number of grid fingers is doubled moving from an inner to an outer zone (the optimum factor[17] is about 1.7). Ring radii are set by letting the difference between ring radii double. The innermost ring radius is 285 microns; the middle ring is at 3 x 285 microns. The last ring at 7 x 285 microns coincides with the circular inner rim of the cell busbar. With these parameters fixed, the number of grid fingers in the outermost zone is numerically optimized assuming uniform 100X AM0 illumination. The optimum was 66, but 72 fingers were used because of mask lay-out considerations. This change makes little difference, as Figure 5 indicates. Theoretical total loss from shadow, grid metal resistance, and emitter sheet resistance is about 6.8%. Computation of these losses is roughly similar in outline to Basore.[16] Grid design parameters and formulae are in Table 2.

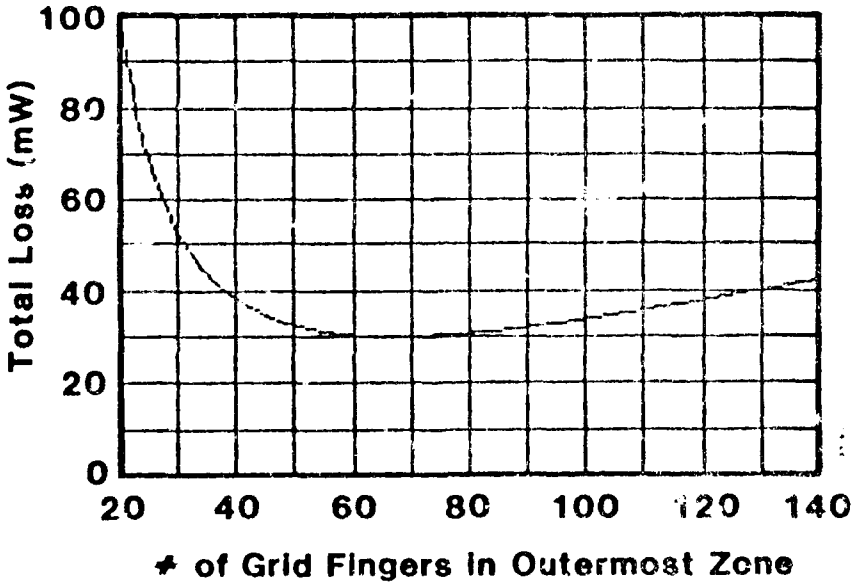

FIGURE 5. TOTAL THEORETICAL LOSS FROM SHADOW, GRID METAL RESISTANCE, AND EMITTER SHEET RESISTANCE AS A FUNCTION OF NUMBER OF FINGERS IN OUTERMOST RING OF GaAs CONCENTRATOR.

TABLE 2. GRID OPTIMIZATION PARAMETERS AND FORMULAE.

PARAMETERS			
V_{max}	1.05	V	Voltage at maximum power point
Q	3.4	A/cm^2	100X AM0 Photogenerated carrier density
w	3	um	Metal grid finger width
δ	2	um	Additional shadow
t	3	um	Metal grid finger width
d	285	um	Innermost ring radius: Middle ring at 3d: 7d = cell radius
T	0.5	um	Thickness of P GaAs emitter layer
R_e	0.015	ohm-cm	Sheet resistivity of P GaAs emitter
R_m	$3x10^{-6}$	ohm-cm	Sheet resistivity of Au grid metal

OPTIMIZED VARIABLE IS NUMBER OF GRID FINGERS (N)

Optimum N is 66
N used was 72

N grid fingers in outermost zone
N/2 fingers in middle zone
N/4 fingers in innermost zone

		P_{loss}	P_{loss}/P_{ava}
Available Power (P_{ava}):	$VQ\pi(7d)^2$ = 446 mW		
Shadow Loss:	$VQ(w+\delta)d(8\pi + 5.25\ N)$	20.5 mW	4.6%
Grid Loss:	$33656(R_m Q^2 d^5)/N\ w\ t)$	3.4 mW	0.8%
Emitter Loss:	$13715(R_e Q^2 d^4)/(N^2 T)$	6.1 mW	1.4%

Total loss (100X AM0): 6.8%

4.0 Ge-UNDER-GaAs BOTTOM CELLS

In this section, we will first describe two experiments to determine whether the long-wavelength photoresponse seen from the Ge bottom cell is due to a p-n junction in the Ge or a heterojunction at the GaAs/Ge interface. Then we will describe average 100X AM0 cell data from Ge cells under heavily-doped P GaAs identical in appearance to the top cell in Figure 3. The cross-sections for these cells are given in Figure 2c. These cells mimic the bottom cell of a tandem, as explained in Section 1. We found evidence that a Ge junction is formed when a GaAs layer is grown on the Ge, as discussed in Section 2.

One question that arises in analyzing the behavior of the bottom cell of the tandem is whether a p-n junction in the n-type Ge substrate causes the photoresponse seen at long wavelengths, or whether this response is due to a heterojunction at the GaAs/Geinterface. Most early work on GaAs/Ge interfaces assumed that observed rectification was due solely to a heterojunction. If, as is quite likely, Ga and As from the GaAs diffuse into Ge during growth, there is a possibility of p-n Ge junction formation since Ga is a p-dopant and As is an n-dopant in Ge. For example, in the pioneering GaAs/Ge paper by Anderson,[19] all effects are attributed to heterojunctions, even though Ga and As diffusion is likely at typical Ge growth temperatures (700°C). Because Anderson's growth conditions (Ge was grown on GaAs, not GaAs on Ge) and surfaces are unlike those in this and similar work,[1,5] we suggest comparisons are of limited use since heterojunction characteristics depend greatly on the interface states, which are almost certainly different. However, from the comparison of (P)GaAs/Ge and (N)GaAs/Ge cells discussed below and previous spreading resistance and EBIC measurements[1,11] indicating a p-n junction in the Ge, we believe that in our present process a Ge p-n junction is mainly responsible for rectifying effects and photovoltage.

To help resolve this issue, we decided to compare results from N GaAs on Ge with P GaAs on Ge. There are two possibilities for the heterojunction theory. If Ga diffusion into Ge from the GaAs growth creates p-Ge near the surface through compensation, the N-p anisotype heterojunction of the N GaAs/Ge cells should presumably have a higher barrier height than the P-p isotype heterojunction of the P GaAs/Ge cells. The I-V curves and photoresponse should then be markedly different. The second possibility, which we feel is unlikely, is if the Ga diffusion into Ge is either electrically inactive or insufficient to compensate the n Ge. However, even in this case, the N-n isotype heterojunction of the N GaAs/Ge cells and the P-n anisotype heterojunction of the P GaAs/Ge cells should again have different IV curves and photoresponse.

In the p-n junction theory, which we strongly support, if a p-n Ge junction is dominant, the I-Vs and photoresponse should be similar for both the P and N GaAs-on-Ge cells. The Ge junction formation depends on diffusing Ga and As, but not on the GaAs dopant atoms, whose concentrations are four orders of magnitude less than the Ga and As atoms from the GaAs. The theory of the Ge p-n junction formation has already been described in Section 2. The p-n junction theory requires an ohmic interface between the N GaAs and p Ge. We believe a tunnel junction occurs since the N GaAs is heavily

doped (2 x $10^{18}/cm^3$) in excess of the effective density-of-states of N GaAs (4.7 x $10^{17}/cm^3$), as is the p Ge (about $10^{20}/cm^3$) above its effective density-of-states ($10^{19}/cm^3$), so that both are degeneratively doped, while the heavy doping on both sides of the interface cause a small depletion region, the necessary conditions for tunneling. Other groups have extensively characterized similar tunnel junctions.[20]

Note that GaAs/Ge heterojunctions exist in both theories; the question is whether the heterojunction barrier height is large enough to affect or dominate the I-V and photoresponse of thebottom cell, or whether a Ge p-n junction is responsible.

In the first experiment, heavily doped GaAs P (#5209-1599) and N (#5209-1600) layers (with no GaAs p-n junction) were grown on Eagle-Picher n-type Ge substrates. The GaAs was doped as heavily as was possible in both cases to minimize any front contact effects. The one-sun 0.25 cm^2 cells we fabricated from these wafers received a sub-optimal AR coating of about 670A ZnS and 930A MgF_2. This lowered the J_{sc}'s for these cells compared to the concentrator cells reported later in this section. However, the inferior AR coating was applied to both cell wafers in the experiment and does not influence the question of whether a heterojunction or a p-n junction is responsible for photodetection. I-V traces of the two cell types are shown in Figure 6a (P GaAs on Ge) and Figure 6b (N GaAs on Ge). Both show a built-in voltage of about 250 mV, consistent with Ge junctions, and a low soft breakdown in the reverse direction of about 300 mV, also consistent with heavily doped junctions. The I-V curves for both of the structures from Figure 2c depicted in Figure 6 are nearly identical. Cell efficiency data were taken with a Spectrolab X-25 simulator and a SERI-calibrated reference cell from the same process lot (Table 3). Typical quantum efficiency curves for the two cell types are shown in Figures 7a (P GaAs on Ge) and 7b (N GaAs on Ge), along with the j_{sc}'s from the integrated quantum efficiency.

The IVs and cell characteristics are quite similar for the P GaAs on Ge and the N GaAs on Ge cells, which would be expected if a p-n Ge junction was responsible for photodetection, but not if a heterojunction was dominant. There is a 11% higher J_{sc} for the N GaAs on Ge cell. This difference is mostly due to the better red response in Figure 7 of the N GaAs on Ge cell, which we attribute to free carrier absorption in the

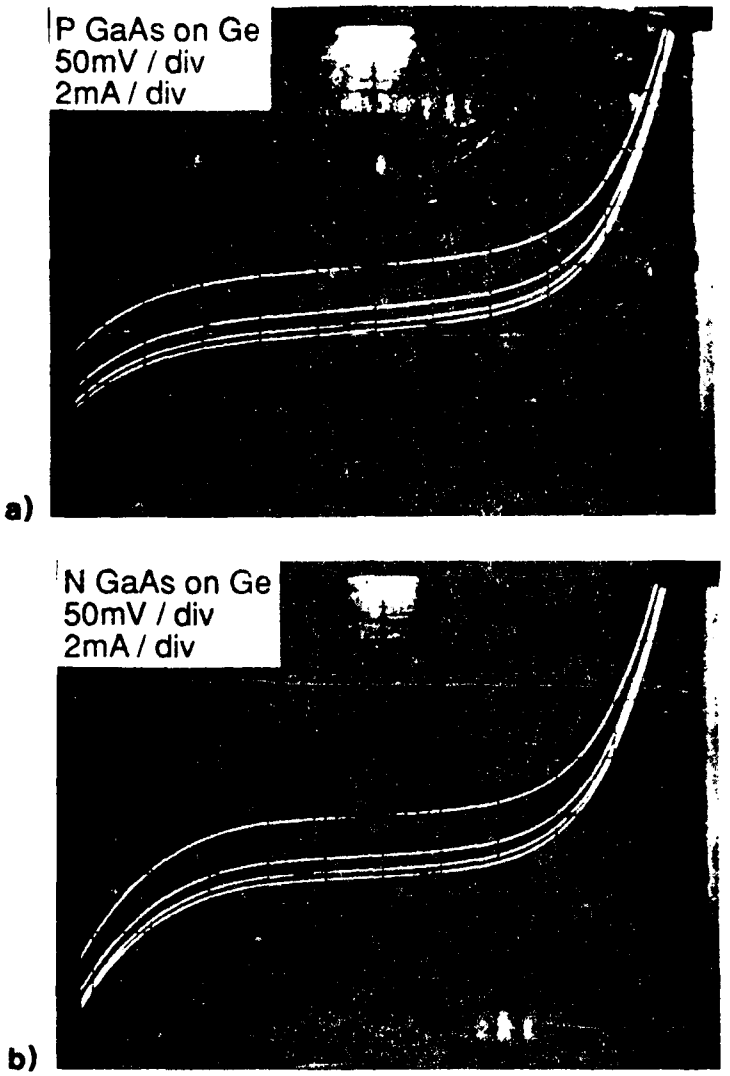

FIGURE 6. I-V CURVES. Origin at center. Uppermost curve is dark IV, lower curves with varying amounts of light from a microscope illuminator. (a) I-V curve of P GaAs on Ge structure; (b) I-V curve of N GaAs on Ge structure.

TABLE 3. AVERAGE ONE-SUN AM0 P AND N GaAs ON Ge DATA.

Wafer	V_{OC} (V)	J_{SC} (mA/cm^2)	Fill Factor %	Efficiency %
P GaAs on n Ge 5209-1599AR (6 cells)	0.214	19.79	56.6	1.71
N GaAs on n Ge 5209-1600AR (4 cells)	0.205	21.42	48.4	1.55
Ref: AM0 137.2mW/cm 25°C				

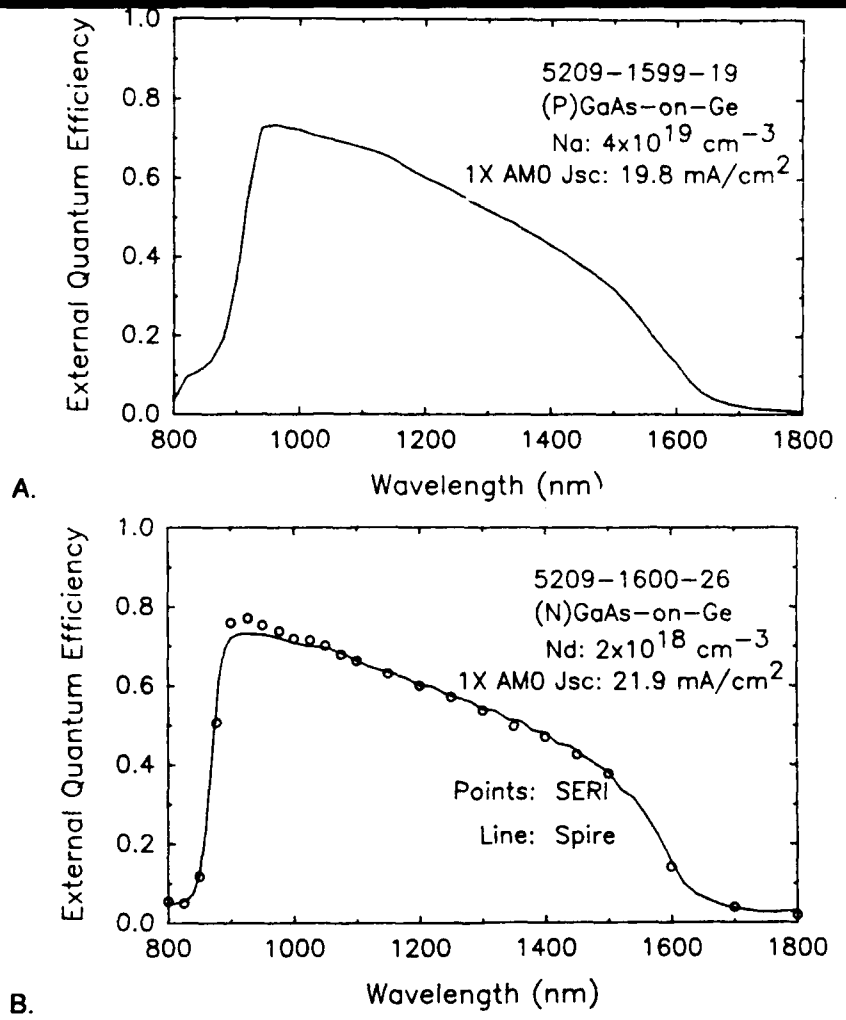

FIGURE 7. QUANTUM EFFICIENCY DATA. J_{SC}'s obtained by integrating quantum efficiency curve with AM0 spectrum. (a) (P)GaAs on Ge structure; (b) (N)GaAs on Ge structure. AR-coating is not optimum for cells.

heavily doped P GaAs. The doping is 20X higher in the P GaAs than the N GaAs. The absorption coefficient for N GaAs below bandgap varies with photon energy, but for a good part of the spectrum is about 10/cm for $2 \times 10^{18}/cm^3$ N GaAs and 300/cm for $5 \times 10^{19}/cm^3$ P GaAs.[18] About 17% fewer photons are available after traversing 6 microns of the P GaAs than exist after 6 microns of the N GaAs. Because of the similarities in the I-V curves and photoresponse of the P and N GaAs-on-Ge cells, we believe the response from the bottom cell must be due to a p-n junction in the Ge, and not to a heterojunction, which should have given different results for the two different structures. This agrees with our previous spreading resistance and cross-sectional EBIC measurements indicating the presence of a Ge p-n junction.[1,5,11] We would like to emphasize that the characteristics of the p-n junction are sensitive to the conditions of the GaAs growth. There have been reports[21] of MOCVD growth temperatures being lowered during the GaAs growth on Ge in order to make the bottom cell inactive; this is predictable in the p-n junction theory since no significant Ga diffusion would occur at low temperatures.

In a second experiment, GaAs was selectively etched off of one Ge wafer with a room temperature 1% Br in methanol etch (etch rate of 1 micron/min at 28°C). This etch of the GaAs removes any possibility of a GaAs/Ge heterojunction. We experimentally confirmed that this etch does not attack Ge, and etched long enough (15 min) to remove all possible GaAs residue. The removal of the GaAs layers is easily visible as there is a color difference between Ge and GaAs. Concentrator cells were fabricated and tested in the same manner as those described in the third experiment below. As expected, these cells still have photoresponse, which can now only be due to a Ge p-n junction since no GaAs remains. A quantum efficiency of an AR coated Ge cell is shown in Figure 8. The dip at 500 nm is due to reflectance. The complete removal of the GaAs was confirmed by Auger analysis. Within its detection limits of about 3 atomic percent, no As or Ga was detected. Also as expected, these cells have a higher efficiency and J_{sc} than Ge-under-GaAs cells since the Ge junction is now not filtered by the GaAs. The response of these cells is reported in Table 4. Since removal of the GaAs should remove any possibility of a heterojunction, this experiment provides definitive proof that the photoresponse of the bottom cell is not from a heterojunction.

TABLE 4. AVERAGE 100X AM0 Ge-UNDER-GaAs BOTTOM CELL DATA.

Wafer	V_{oc} (V)	J_{sc} (mA/cm^2)	Fill %	Efficiency %	Number Tested
P GaAs on Ge Vendor 1 $2.6 \times 10^{17}/cm^3$	0.318	2843.8	62.3	4.12	17
P GaAs on Ge Vendor 2 $6 \times 10^{16}/cm^3$	0.316	2688.8	59.6	3.67	11
P GaAs on Ge Vendor 3 $3.3 \times 10^{17}/cm^3$	0.315	2853.1	59.1	3.88	10
No GaAs on Ge Vendor 1 $2.6 \times 10^{17}/cm^3$	0.311	4389.2	59.1	5.84	4
Ref: AM0 137.2mW/cm^2					

In a third experiment, P GaAs was grown on Ge substrates from several vendors, and concentrator cells (#5224) were made. We wished to see how substrates from different vendors (and therefore presumably with different minority carrier lifetimes) affect the lifetime and diffusion lengths of these carriers, and therefore the bottom cell efficiency. The P GaAs on Ge structure was selected for this experiment to avoid any tunnel resistance effects from N GaAs/p Ge junctions. The AR coating of 900A ZnS and 1500A MgF_2 was designed to maximize the photocurrent from the Ge cell and match photocurrents from the top and bottom cells of a tandem. Another difference from the one-sun #5209 cells in Table 3 was that most of the p-GaAs layer was doped to $5x10^{17}/cm^3$ to reduce free-carrier absorption, with thin heavily doped layers at the front surface and Ge interface to assure low-resistance contacts.

Results from testing with a SERI-calibrated GaAs/Ge reference and a Spectrolab X-25 simulator are in Table 4. The test block temperature was 25°C, but the cell surface was probably 10-13°C hotter at concentration. The simulator intensity was set so that the one-sun current from the GaAs/Ge reference cell matched its AM0 value. The concentrators were then measured at one-sun, and the simulator intensity was increased with a Fresnel lens to achieve 100X the one-sun J_{sc}. The J_{sc} was assumed to be linear with light intensity. The best P GaAs on Ge cells were 4.6% efficient at 100X AM0. One-sun J_{sc}'s obtained by integrating the quantum efficiency with the AM0 spectrum range from 26.1 to 31.0 mA/cm^2 for the (P)GaAs/Ge concentrators, and from 37.4 to 41.9 mA/cm^2 for the Ge concentrators without GaAs, in reasonable agreement with the simulator-measured J_{sc}'s.

As shown in Table 4, there is a small difference in efficiency among different Ge substrate vendors, which may be due either to material quality or differences in doping. Within several microns of the Ge p-n junction, the n type base doping is dominated by As diffusing from the GaAs and substrate doping is small compared to the diffused As, so the substrate doping plays little part in the area adjacent to the Ge p-n junction. However, the absorption length of 1550-1850 nm light in Ge is fairly long, 10 to 500 microns, so that most of the photons should be absorbed away from the As diffusion tail caused during GaAs growth. This tail is harmful since it creates a potential gradient which pushes minority carriers away from the junction. Photogenerated electron-hole pairs from longer wavelength photons must diffuse back to the junction against this tail in order to be collected. Their success in accomplishing this is related to their lifetime, which depends on the substrate doping and quality.

A quantum efficiency from one of these concentrators (#5224-7-14B) is shown in Figure 8. The tail extending from 300 to 850 nm in the plot was unexpected but is real. Almost all the photons in this spectral range are absorbed in the GaAs. One possible theory is that some of the carriers generated in the GaAs are able to diffuse through the 6 micron GaAs and be collected in the Ge junction. The GaAs in these #5224 concentrator cells were more lightly doped than in the #5209 one-sun cells of Figure 8. ($5x10^{17}/cm^3$ vs. $5x10^{19}/cm^3$).

This report is substantially the same as the work reported in reference 22.

REFERENCES

1. S.P. Tobin et al. "High Efficiency GaAs/Ge Monolithic Tandem Solar Cells," in Conf. Rec. 20th IEEE Photovoltaic Specialists Conf., 1988, pp.405-410.

2. K.I. Chang, Y.C.M. Yeh, P.A. Iles, J.M. Tracy, and R.K. Morris, "Heterostructure GaAs/Ge Solar Cells," in Conf. Rec. 19th IEEE Photovoltaic Specialists Conf., 1987, pp. 273-279.

3. L.D. Partain, H.F. MacMillan, G.F. Virshup, and N.R. Kaminar, "Quantum Yield Spectra and I-V Properties of a GaAs Solar Cell Grown on a Ge Substrate," late news paper in Conf. Rec. 20th IEEE Photovoltaic Specialists Conf., 1988, pp.759-763.

4. B.T. Cavicchi, D.R. Lillington, G.F.J. Garlick, G.S. Glenn, and S.P. Tobin, "GaAs on Ge Cell and Panel Technology for Advanced Space Flight Application," in Conf. Rec. 20th IEEE Photovoltaic Specialists Conf., 1988, pp.918-923.

5. S.P. Tobin, S.M. Vernon, C. Bajgar, V.E. Haven, L.M. Geoffroy, and D.R. Lillington, "High Efficiency GaAs/Ge Monolithic Tandem Solar Cells," IEEE Electron Device Lett., Vol. EDL-9, pp. 256-258, 1988.

6. K. Emery and C. Osterwald, "AM0 Efficiency Measurements," NASA SPRAT, April 1988, pp. 352-353.

7. K. Emery, C. Osterwald, T. Glatfelter, J. Burdick, and G. Virshup, "A Comparison of the Errors in Determining the Conversion Efficiency of Multi-Junction Solar Cells by Various Methods," Solar Cells, Vol. 24, 1988, pp. 371-380.

8. R.E. Hart, D.J. Brinker, and K.A. Emery, "High Altitude Current-Voltage Measurement of GaAs/Ge Solar Cells," in Conf. Rec. 20th IEEE Photovoltaic Specialists Conf., 1988, pp.764-765.

9. F.A. Trumbore "Solid Solubilities of Impurity Elements in Germanium and Silicon," Bell Sys. Tech. Jour., 1960, pp. 205-233.

10. S.M. Sze, Physics of Semiconductor Devices, 2nd Ed., Wiley, 1981, pp. 68.

11. S.P. Tobin and S.M. Vernon, "High Efficiency GaAs and GaAs/Ge Tandem Solar Cells," Proc. of 4th International Photovoltaic Science and Engineering Conference, Sydney, Australia, 1989, pp.865-872.

12. S.P. Tobin et al., "Assessment of MOCVD- and MBE-Grown GaAs for High-Efficiency Solar Cell Applications," submitted to IEEE T-ED, this issue.

13. "Standard for Terrestrial Direct Normal Solar Spectral Irradiance Tables for Air Mass 1.5," ASTM Standard E891-87, 1988 (American Society for Testing of Materials, Philadelphia, PA).

14. H.F. MacMillan, N.R. Kaminar, M.S. Kuryla, M.J. Ladle, D.D. Liu, and G.F. Virshup, "28% Efficient GaAs Concentrator Solar Cells," Conf. Record of the 20th IEEE Photovoltaic Specialists Conf., 1988, pp.462-468.

15. R.A. Sinton, Y. Kwark, J.Y. Gan, and R.M. Swanson, "27.5-Percent Silicon Concentrator Solar Cells," IEEE Electron Dev. Lett., Vol. EDL-7, pp. 567-569, 1986.

16. P.A. Basore, "Optimum Grid-Line Patterns for Concentrator Solar Cells Under Non-Uniform Illumination," Solar Cells, Vol.14, 1985, pp. 249-260.

17. S.P. Tobin, "Development of a Thin AlGaAs Solar Cell," Sandia Report SAND87-7098, Appendix A, Nov. 1985.

18. H.C. Casey, D.D. Sell, and K.W. Wecht, "Concentration Dependence of the Absorption Coefficient for n and p type GaAs between 1.3 and 1.6 eV," Journal of Applied Physics, Vol. 46, No. 1, Jan. 1975, pp. 250-257.

19. R.L. Anderson, "Experiments on Ge-GaAs Heterojunctions," Solid State Electronics, Vol. 5, 1962, pp. 341-351.

20. M.L. Timmons, J.A. Hutchby, D.K. Wagner, and J.M. Tracy, "Monolithic AlGaAs/Ge Cascade Solar Cells," Conf. Record of the20th IEEE Photovoltaic Specialists Conf., 1988, pp.602-606.

21. P.A. Iles, F. Ho, M. Yeh, G. Datum, and S. Billets, "Gallium Arsenide-on-Germanium Solar Cells," 24th Intersociety Energy Conversion Engineering Conference, 1989, pp.791-797.

22. S.J. Wojtczuk, S.P. Tobin, C.J. Keavney, C. Bajgar, M.M. Sanfacon, L.M. Geoffroy, T.M. Dixon, S.M. Vernon, J.D. Scofield, D.S. Ruby, "GaAs/Ge Tandem-Cell Space Concentrator Development," IEEE Transactions on Electron Devices, Vol. 37, No. 2, February 1990, pp. 455-463.

Steven J. Wojtczuk
Principal Investigator

U.S. Government Printing Office 548-076